Tyrosine-48 Is the Proton Donor and Histidine-110 Directs Substrate Stereochemical Selectivity in the Reduction Reaction of Human Aldose Reductase: Enzyme Kinetics and Crystal Structure of the Y48H Mutant Enzyme[†,‡]

Kurt M. Bohren,[§] Charles E. Grimshaw,[∥] Chung-Jeng Lai,[∥] David H. Harrison,[⊥] Dagmar Ringe,[⊥] Gregory A. Petsko,[⊥] and Kenneth H. Gabbay*[,§,⊥]

Molecular Diabetes and Metabolism Section, Departments of Pediatrics and Cell Biology, Baylor College of Medicine, Houston, Texas 77030, The Whittier Institute for Diabetes and Endocrinology, La Jolla, California 92037, and The Rosenstiel Basic Medical Sciences Research Center, Brandeis University, Waltham, Massachusetts 02554

Received October 11, 1993; Revised Manuscript Received December 13, 1993[⊛]

ABSTRACT: The active site of human aldose reductase contains two residues, His110 and Tyr48, either of which could be the proton donor during catalysis. Tyr48 is a candidate since its hydroxyl group is in proximity to Lys77 and thus may have an abnormally low pK_a value. To distinguish between these possibilities, we used site-directed mutagenesis to create the H110Q and H110A, the Y48F, Y48H, and Y48S, and the K77M mutant enzymes. The two His110 mutants resulted in a 1000–20 000-fold drop in k_{cat}/K_m, respectively, for the reduction of DL-glyceraldehyde at pH 7. The Y48F mutation caused total loss of activity, whereas the Y48H and Y48S mutants retained catalytic activity with k_{cat}/K_m reduced by 5 orders of magnitude. The K77M mutant is an inactive enzyme. Kinetic studies using xylose stereoisomers show that the wild-type enzyme distinguishes between D-xylose, L-xylose, and D-lyxose up to 150-fold better than the H110A or H110Q mutants. The His110 mutants do not effectively discriminate between these isomers (4–11-fold). The crystal structure of the Y48H mutant refined at 1.8-Å resolution shows that the overall structure is not significantly different from the wild-type structure. Electron densities for the histidine side chain and a new water molecule fill the space occupied by Tyr48 in the wild-type enzyme. The water molecule is in hydrogen-bonding distance to the Nζ group of Lys77 and to the Nϵ of His48 and fills the space occupied by the hydroxyl group of tyrosine in the wild-type structure. These findings suggest that proton transfer is mediated in the Y48H mutant enzyme by the water molecule. The Y48H mutant shows large and equal primary deuterium isotope effects on k_{cat} and k_{cat}/K_m (1.81 ± 0.03), providing direct evidence for hydride transfer as the rate-determining step in this mutant. Deuterium solvent isotope effects indicate that the relative contribution of proton transfer to this step of the catalytic cascade is much less important for the Y48H mutant than for the wild-type enzyme [$^{D_2O}(k_{cat}/K_m)$ = 1.06 ± 0.02 and 4.73 ± 0.23, respectively]. The kinetic and mutagenesis data, together with structural data, indicate that His110 plays an important role in the orientation of substrates in the active site pocket, while Tyr48 is the proton donor during aldehyde reduction by aldose reductase.

Aldose reductase (EC 1.1.1.21), a member of the aldo–keto reductase superfamily (Bohren et al., 1989), catalyzes the NADPH-dependent reduction of a wide range of carbonyl compounds such as sugars, aldehyde metabolites, corticosteroid hormones, and a variety of xenobiotic aldehydes (Wermuth, 1985). Interest in this enzyme stems in part from its ability to reduce glucose and galactose causing diabetic and galactosemic complications affecting the lens, retina, nerves, and kidneys (Gabbay, 1973; Kador, 1988). A number of aldose reductase inhibitors (ARIs) have been developed and tested in patients for the treatment of such complications (Gabbay et al., 1979; Judzewitsch et al., 1983; Dvornik, 1987; Stribling et al., 1989; Masson & Boulton, 1990). Presently, none of these drugs are therapeutically effective due to their side effects, nonspecificity, and inhibition of other members of the aldo–keto reductase family (Martyn et al., 1987; O'Brien et al., 1982; Poulsom, 1986).

In order to develop a rational basis for the design of specific inhibitors of aldose reductase, it is important to understand the mechanism of enzymatic catalysis. To aid in this aim, we have crystallized and determined the refined X-ray crystallographic structure of human aldose reductase (Wilson et al., 1992; Harrison et al., 1994). Currently, it is thought that the mechanism proceeds through a hydride-transfer step followed or preceded by a proton-transfer step. The enzyme active site contains two residues, Tyr48 and His110, either of which could function as the proton donor during the protonation of the carbonyl oxygen of the substrate. Tyr48 appears to be a likely candidate. In the structure of the wild-type enzyme, the oxygen

[†] This work was supported by grants from the National Institutes of Health (DK-39044, DK-43595, and GM-26788), the Juvenile Diabetes Foundation, the Lucille P. Markey Charitable Trust, the Charles E. Culpeper Foundation, and the Harry B. and Aileen B. Gordon Foundation. Part of this work was done during a sabbatical by K.H.G. as Visiting Scientist in the laboratory of D.R. and G.A.P. (1992–1993).

[‡] The atomic coordinates and structure factors have been deposited in the Brookhaven Protein Data Bank (reference: 1ACU = Y48H mutant enzyme–NADP$^+$–citrate).

* Address correspondence to this author at the Departments of Pediatrics and Cell Biology, Baylor College of Medicine, 1 Baylor Plaza, Houston, TX 77030 [telephone (713)770-3765; FAX (713)770-3766; internet kgabbay@mbcr.bcm.tmc.edu].

[§] Baylor College of Medicine.

[∥] The Whittier Institute for Diabetes and Endocrinology.

[⊥] Brandeis University.

[⊛] Abstract published in *Advance ACS Abstracts,* February 15, 1994.

0006-2960/94/0433-2021$04.50/0

Table 1: Oligonucleotide Primers Used for Site-Directed Mutagenesis[a]

H110A	5′ CTACCTTATTGCCTGGCCGACTGGC 3′
H110Q	5′ CTACCTTATTCAGTGGCCGACTGGC 3′
Y48H	5′ GCCCATGTGCACCAGAATGAGAAT 3′
Y48S	5′ GCCCATGTGTCCCAGAATGAGAAT 3′
Y48F	5′ GCCCATGTGTTCCAGAATGAGAAT 3′
K77M	5′ CATCGTCAGCATGCTGTGGTGCAC 3′

[a] Underlined letters indicate base change.

of the tyrosine hydroxyl is located 3.1 Å from the Nζ of Lys77, and this interaction could facilitate proton transfer from the tyrosine to the substrate. His110 is surrounded by three adjacent hydrophobic residues with its Nε within 5 Å of the Nζ of Lys77. This environment is expected to lower the pK_a of histidine sufficiently so that the side chain is not protonated at physiological pH. In order to determine the roles of His110 and Tyr48, we made several mutant enzymes by changing Tyr48 to Phe (Y48F), to His (Y48H), and to Ser (Y48S) and changing His110 to Gln (H110Q) and Ala (H110A). In addition, the critical hydrogen-bonding interaction of the ammonium group of Lys77 with the hydroxyl of Tyr48 was examined by mutation of the Lys77 residue to methionine (K77M). Enzyme kinetic studies of these mutants were carried out in conjunction with crystallographic studies. The Y48H mutant enzyme was readily crystallized and its structure determined by molecular replacement and refinement at 1.76-Å resolution. The combined structure–function data indicate that His110 plays a major role in orienting 2-hydroxyaldehyde substrates in the active site pocket, while Tyr48 is indeed the proton donor in the aldehyde reduction reaction catalyzed by aldose reductase.

MATERIALS AND METHODS

Plasmid Construction and Production of Protein. The aldose reductase cDNA (Bohren et al., 1989) was subcloned into M13mp18 using the *Eco*RI restriction sites. Mutagenesis was done by using the Amersham Corp. *in vitro* mutagenesis system (version 2.1) and primers shown in Table 1. cDNAs bearing the various mutations were introduced into pET11a using the polymerase chain reaction (PCR) as previously described (Bohren et al., 1991) with modified primers: The two primers carrying the *Nde*I site were elongated by seven nucleotides on their 5′ end to improve the cutting efficiency of the restriction enzyme. To minimize PCR copying errors of the templates, 15 cycles or less were carried out using Vent polymerase (New England Biolabs), which has proofreading activity. The oligonucleotide primers were synthesized by National Biosciences (Plymouth, MN), and all constructs were completely sequenced (Sequenase kit, United States Biochemicals) to verify the desired mutations and ensure that no other mutations had occurred. The recombinant plasmids were overexpressed and the resulting proteins purified as described in detail elsewhere (Bohren et al., 1991). In cases where the expressed protein had extremely low activity under standard assay conditions, the eluants from the chromatography columns were monitored by SDS–polyacrylamide gel electrophoresis.

SDS–Polyacrylamide Gel Electrophoresis and Isoelectric Focusing. SDS–polyacrylamide gels were run on precast 10–15% gradient gels or 20% homogeneous gels on the Phastsystem (Pharmacia) in the presence of 2% β-mercaptoethanol (β-ME)[1] as described by the manufacturer. Isoelectric focusing was carried out using precast gels (pH 3–9) according to the manufacturer's (Pharmacia) instructions. The protein concentration of purified enzymes was determined with the Bio-Rad protein assay kit, using bovine γ-globulin as the standard.

Enzyme Assays and Kinetic Analyses. Enzymatic activities were assayed during purification by measuring the rate of the enzyme-dependent decrease of NADPH absorption at 340 nm in either a Gilford Response or a Cary 3 spectrophotometer at 25 °C. The standard reaction mixture (1-mL volume) contained 0.2 mM NADPH and 1–10 mM DL-glyceraldehyde, depending on the mutant enzyme being analyzed, in a 100 mM sodium phosphate buffer, pH 7. Kinetic constants were determined in the same way except the substrate or cofactor concentrations were varied. Each data point (initial velocity) was determined in duplicate over at least six different substrate concentrations. Control assays, lacking either substrate or enzyme, were routinely included, and the rates, if any, were subtracted from the reaction rates. Kinetic constants were calculated by fitting the Michaelis–Menten function directly in the hyperbolic form to the data with an unweighted least-squares analysis using the Marquardt–Levenberg algorithm provided with SigmaPlot, version 5.1. In cases where substrate inhibition occurred, the Michaelis–Menten function was modified to the equation

$$v_i = VA/(K_m + A + A^2/K_i) \quad (1)$$

where v_i is the initial velocity, A is the substrate concentration, V is the apparent maximal velocity, K_m is the apparent Michaelis–Menten constant, and K_i is the apparent substrate inhibition constant. Steady-state kinetics in the presence of inhibitors were analyzed by using the equation

$$v_i = VA/[K_m(1 + I/K_{is}) + A(1 + I/K_{ii})] \quad (2)$$

where K_{is} is the slope (competitive) inhibitory constant and K_{ii} is the intercept (uncompetitive) inhibition constant. The inhibition pattern and a >5-fold relative difference between K_{is} and K_{ii} determined competitive or uncompetitive inhibition. Accordingly, either term in the equation was set to 1, and the fit for either K_{is} or K_{ii} improved significantly, as judged from the standard errors and the sum of the residual least-squares values. The kinetic nomenclature used is that of Cleland (1963).

Determination of pH Profiles. pH profiles were determined over the range of pH 5–10 using the following buffers: MES (pH 5–6.5), MOPSO (pH 6.5–7.5), POPSO (pH 7.5–8.5), CHES (pH 8.5–9.5), and CAPSO (pH 9.5–10).[1] Overlaps were used in all cases, and checks were made to ensure that none of the buffers were inhibitory. For k_{cat} and k_{cat}/K_m pH profiles using DL-glyceraldehyde, the nucleotide concentration used was in all cases shown to be saturating (at least 10 × K_m). The pH profiles for k_{cat} and k_{cat}/K_m were fitted to eq 3–5, which describe log Y vs pH curves that decrease above pK_1 (eq 3), that decrease both below pK_1 and above pK_2 (eq 4), and that go through a wave, decreasing at high pH above pK_1, leveling off at pK_2, and decreasing again above pK_3 (pK_3 > pK_2 > pK_1; eq 5), respectively. In eq 3–5, Y is k_{cat} or k_{cat}/K_m, H is [H$^+$], and Y_{max} is the value of Y at the optimal state of protonation. The points in Figure 3 are the experimentally determined values, while the curves are

[1] Abbreviations: MES, 2-(*N*-morpholino)ethanesulfonic acid; MOPSO, 3-(*N*-morpholino)-2-hydroxypropanesulfonic acid; POPSO, piperazine-*N*,*N*′-bis(2-hydroxypropanesulfonic acid); CHES, 2-(*N*-cyclohexylamino)ethanesulfonic acid; CAPSO, 3-(cyclohexylamino)-2-hydroxy-1-propanesulfonic acid; PEG, poly(ethylene glycol); β-ME, β-mercaptoethanol.

calculated from fits of these data to the appropriate equations:

$$\log Y = \log[Y_{max}/(1 + K_1/H)] \quad (3)$$

$$\log Y = \log[Y_{max}/(1 + H/K_1 + K_2/H)] \quad (4)$$

$$\log Y = \log[Y_{max}(1 + K_2/H)/(1 + (K_1/H)(1 + K_3/H))] \quad (5)$$

Studies of Isotope and Solvent Effects. NADPH and NADPD labeled with deuterium in the *pro-R* position were synthesized from unlabeled and 2-deuterio-L-malate using malic enzyme by the method of Viola et al. (1979) and were purified by FPLC on a Mono-Q column using the procedure of Orr and Blanchard (1984). A value for $^{D}k_{cat} = 1.00$ observed under conditions where $NADP^+$ release is the rate-limiting step for k_{cat} (Grimshaw et al., 1989) confirms the lack of inhibitory impurities in the NADPH and NADPD samples (Cleland, 1979). Primary deuterium isotope effects[2] on k_{cat} and k_{cat}/K_m for DL-glyceraldehyde were measured by direct comparison at saturating NADPH/D concentrations in 50 mM MOPSO (pH 7.0) buffer at 25 °C. Initial velocities, corrected for background, were fitted to the equation

$$v_i = VA/[K_m(1 + F_iEk_{cat}/K_m) + A(1 + F_iEk_{cat})] \quad (6)$$

where F_i is the fraction of deuterium in the NADPH/D cofactor, Ek_{cat}/K_m and Ek_{cat} are the isotope effects minus 1 on k_{cat}/K_m and k_{cat}, respectively, and the other kinetic parameters are as described above, by the nonlinear least-squares method and using the Fortran programs of Cleland (1979). In those cases where the Ek_{cat} value appeared to be 0 (i.e., no isotope effect on k_{cat}), the data were fitted to the equation

$$v_i = VA/[K_m(1 + F_iEk_{cat}/K_m) + A] \quad (7)$$

For the Y48H mutant in particular, where Ek_{cat}/K_m and Ek_{cat} appeared to be identical, the data were fitted to the equation

$$v_i = VA/[(K_m + A)(1 + F_iE)] \quad (8)$$

where we assume $E = Ek_{cat}/K_m = Ek_{cat}$. In each instance, the criteria for deciding if a particular E value was significantly different from 0 were, first, to compare the fitted value with its standard error and, second, to compare the residual least-squares value, or its square root, SIGMA, obtained from a fit to the equation containing the E value in question (e.g., Ek_{cat} in eq 6) to that obtained from the fit where $E = 1.00$ (e.g., $Ek_{cat} = 1.00$ in eq 6). Adding extra terms to a rate equation will lower SIGMA only when the fit is actually improved (Cleland, 1979).

Solvent isotope effects on k_{cat} and k_{cat}/K_m for DL-glyceraldehyde were measured in a similar manner by direct comparison of initial velocities determined at a saturating NADPH concentration. Buffers made in D_2O were adjusted with NaOD to the desired "pH" using a formula (pD = meter reading + 0.4) that corrects for the isotope effect on the response of the glass electrode (Salomaa et al., 1964). Initial velocity data were similarly fitted to eq 6–8, as appropriate, using F_i to correct for the mole percent of D_2O used.[3] DL-Glyceraldehyde stock solutions in H_2O and D_2O were in all cases calibrated by means of end-point assays with excess wild-type enzyme to ensure accurate determination of the solvent Ek_{cat}/K_m effect.

Circular Dichroism Spectroscopy. CD spectra were measured over the range of 190–260 nm in a Jasco (Easton, MD) J-500A spectropolarimeter calibrated with 0.1% *d*-10-camphorsulfonic acid solution. Measurements were made using 50-μm path-length cells and protein concentrations of 1 mg/mL at 25 °C with a 2-s time constant and a scan rate of 25 nm/min. The sampling wavelength was set at 0.2 nm and the spectral bandwidth at 2 nm. Spectra were measured 15 times and averaged.

Proteolytic Fingerprint. Twenty-five microliters of the undenatured sample protein (2.5 mg/mL) was incubated at room temperature with 4 μL of a specific protease (alkaline protease, endoproteinase Glu-C, or endoproteinase Lys-C, each at 0.025 mg/mL; Promega) in 5 mM sodium phosphate, pH 7.4, with 7 mM β-ME and 0.1 mM EDTA. Aliquots were removed after 0.25, 1, 4, and 24 h, analyzed on 20% SDS–PAGE gels, and stained using the Bio-Rad silver stain kit.

Crystallization. Recombinant wild-type and Y48H mutant aldose reductases were crystallized under the same conditions described earlier (Wilson et al., 1992). Numerous attempts to crystallize the Y48F mutant enzyme, over an 18-month period and using more than a dozen different enzyme preparations and a wide range of crystallization conditions, were unsuccessful. Purified protein (15–20 mg/mL) in 25 mM citrate, pH 5.0, containing 7 mM β-ME, 2 mM sodium phosphate, 0.05 mM EDTA, and various concentrations of poly(ethylene glycol) (PEG) 6000, was placed in hanging drops over wells containing 20% PEG in 50 mM citrate, pH 5.0. Wild-type crystals were used as seeds to get Y48H crystals. Crystals were harvested, stored, and shipped in 30% PEG in 50 mM citrate, pH 5.0, prior to mounting. These crystals are isomorphous with those previously reported (Harrison et al., 1994).

Diffraction Data Collection and Structure Refinement. Crystals were directly transferred and mounted in a 0.7-mm quartz capillary. Unaligned crystals were irradiated using an Eliot GX-6 rotating anode (30 kV × 30 mA), and diffraction spot intensities were recorded on a Siemens X-100A multiwire proportional X-ray detector as described in the preceding paper (Harrison et al., 1994). The XDS and XSCALE programs (Kabsch, 1988) were used to integrate and merge the indexed intensities. The R_{merge} statistics and data completeness are summarized in Table 2.

Crystallographic Refinement. We used the phases developed for the native aldose reductase structure described in the preceding paper (Harrison et al., 1994) to arrive at a model of the crystal structure of Y48H. A series of cycles of manual fitting of the model to electron density maps and water molecule search using WATERHUNTER (Sugio, personal communication), followed by positional and individual *B*-factor refinements using XPLOR (Brünger, 1992), were used to refine the model as previously described (Harrison et al., 1994). Table 2 summarizes the statistics and refinement data for the

[2] The isotope effect nomenclature is that of Northrop (1977) in which a leading superscript indicates the isotope effect being studied. Thus, $^{D}k_{cat}$ and $^{D}k_{cat}/K_m$ are primary deuterium isotope effects (that is, values for the hydrogen molecule divided by values for the deuterated molecule) on the respective parameters. Similarly, $^{D_2O}k_{cat}$ and $^{D_2O}k_{cat}/K_m$ are the solvent isotope effects on the same parameters.

[3] Due to the low k_{cat} for Y48H, only an 80% mole fraction of D_2O was used, while a ≥90% mole fraction was used for the wild-type enzyme. Although we have not yet conducted a proton inventory experiment (Schowen, 1978) to confirm a linear relationship between the solvent isotope effect and the mole fraction of D_2O, the anticipated corrections will be well within the experimental error of the measurements and, in any case, will have little effect on interpretation of the results.

Table 2: Data Collection and Refinement Statistics

space group	$P2_12_12_1$
R_{merge}	11.7%
completeness	
∞–6.0 Å	94.1%
6.0–4.5 Å	98.8%
4.5–3.0 Å	98.1%
3.0–2.5 Å	96.0%
2.5–2.0 Å	88.8%
2.0–1.8 Å	40.8%
reflections	
$I/\sigma(I) > 0$	75201
unique	23622
cell dimensions	
a	49.99 Å
b	67.14 Å
c	92.07 Å
refinement resolution	10.0–1.76 Å
R-factor	18.7%
rms deviation from ideal geometry	
bond lengths	0.014 Å
angles	1.54°

Table 3: Apparent Kinetic Constants of Wild-Type Human Aldose Reductase and Its Y48, H110, and K77 Mutants[a]

	DL-glyceraldehyde			*p*-nitrobenzaldehyde		
	K_m (mM)	k_{cat}	k_{cat}/K_m	K_m (mM)	k_{cat}	k_{cat}/K_m
wild type	0.02	0.45	22687	0.004	0.41	92971
H110Q	12	0.25	21	0.86	0.02	23
H110A	84	0.07	0.9	0.19	0.03	146
Y48F		0			0	
Y48H	71	0.01	0.2	0.1	0.01	74
Y48S	64	0.01	0.07	0.88	0.002	2.5
K77M		0			0	

[a] k_{cat} (s^{-1}) and k_{cat}/K_m (s^{-1} M^{-1}) values for AR_{wild} are from Bohren et al. (1991); standard deviation <20%.

Y48H crystal structure (21 974 reflections in the range 10–1.76 Å were used in the refinement). The current model, including 142 bound water molecules, has been refined to an *R*-factor of 18.7% versus all observed data with intensities of $I/\sigma(I) > 1$ in the resolution range 10.0–1.76 Å.

RESULTS

Expression and Purification of Recombinant Proteins. All constructs were readily expressed in the pET system and yielded 20–30 mg of pure protein per 3-L culture. The purified enzymes show single bands on SDS–polycacrylamide gel electrophoresis. Upon isoelectric focusing, the wild-type and all mutant enzymes showed a major band at pH 6.2 with the exception of the K77M mutant, which showed an acidic shift of approximately 0.2 pH unit. The isoelectric points of these recombinant aldose reductases are generally shifted by 0.3 pH unit higher than the isoelectric point of native aldose reductase enzyme due to the unmodified N-termini (Bohren et al., 1991). Charge heterogeneity, noted as more acidic bands, was observed with all purified proteins and is in part caused by the presence of β-ME at all stages of purification (Wermuth et al., 1982; Bohren & Gabbay, 1993).

Characteristics of Mutant Proteins. Steady-state kinetic constants of the various mutant proteins are summarized in Table 3. In general, the k_{cat} values of all the mutant proteins, using either DL-glyceraldehyde or *p*-nitrobenzaldehyde as substrates, were drastically reduced or too small to be measurable. The His110 mutants were affected to a lesser extent than the Tyr48 or Lys77 mutants. Thus, the k_{cat} of the H110Q mutant was reduced to 55% and 5% of the wild-type values obtained for DL-glyceraldehyde and *p*-nitrobenzaldehyde as substrates, and the corresponding K_m values increased 600- and 200-fold, respectively. The k_{cat}/K_m, or catalytic efficiency, dropped to 0.09% and 0.025%, respectively, for the two substrates. The H110A enzyme mutant was also severely affected with k_{cat} decreases to 15% and 7%, K_m increases of 4200- and 50-fold, and k_{cat}/K_m decreases to 0.004% and 0.15% of the wild-type values for the two substrates, respectively. Interestingly, the ratios of the respective k_{cat}/K_m values show that the H110A mutant is more severely affected than the H110Q enzyme with DL-glyceraldehyde as a substrate (H110Q is 22-fold better), while the reverse is true for *p*-nitrobenzaldehyde (H110A is 6-fold better). These findings suggest that the His110 residue may affect substrate accommodation in the active site pocket since the two substrates differ in their relative polarity and hydrophobicity, with DL-glyceraldehyde being a highly polar substrate and *p*-nitrobenzaldehyde representative of the typical hydrophobic substrates of aldose reductase.

The possible role of His110 in determining the stereospecificity of the enzyme with respect to substrates was also examined with D-xylose and its stereoisomers, L-xylose and D-lyxose, as substrates. D-Lyxose is an isomer of D-xylose which differs only in the steric configuration of the hydroxyl group on C2. Native human aldose reductase prefers D-xylose to L-xylose, with the respective K_m values being 5 and 100 mM (Wermuth et al., 1982). The kinetic data for the recombinant wild-type human enzyme and its H110A mutant for D-xylose, L-xylose, and D-lyxose are shown in Table 4.[4] The catalytic efficiency of the wild-type enzyme is 25-fold better for D-xylose than for L-xylose and 900-fold better for D-xylose than for D-lyxose, indicating that the wild-type enzyme is able to differentiate between these isomers. The corresponding catalytic efficiency ratios of the H110A mutant enzyme for these substrate pairs are approximately 4- and 7-fold, respectively. Thus, the absence of stereoselectivity of the H110A enzyme mutant for D-xylose versus L-xylose, and D-xylose versus D-lyxose, measured as the ratio of k_{cat}/K_m values, indicates that this mutant does not discriminate effectively between these isomers. Furthermore, the marked difference in the wild-type enzyme between the D-xylose/L-xylose (25-fold) and D-xylose/D-lyxose (900-fold) catalytic efficiency ratios indicates that the interaction of the substrate with His110 is determined by the configuration of both the C2- and C3-hydroxyl groups. These findings suggest that His110 plays an important role in the stereochemical orientation of 2-hydroxyaldehyde substrates within the active site pocket.

The Tyr48 mutations affected all parameters of enzyme activity to an even greater extent (Table 3). The Y48F mutant was found to be inactive. This mutant was tested at pH ranges from 5 to 8, using up to 0.5 mg of protein per assay, and DL-glyceraldehyde concentrations from 0.1 to 100 mM or *p*-nitrobenzaldehyde concentrations from 0.1 to 2 mM. The K77M mutant was similarly tested and found to have no detectable activity. The complete inactivity of aldose reductase with the Y48F point mutation prompted us to closely examine its physical properties. IEF, SDS–PAGE, and Western blot analyses were unable to distinguish this mutant from the wild-type enzyme. CD spectra (Figure 1) were obtained with the

[4] Although the actual substrate for aldose reductase has been shown to be the free aldehyde form (Grimshaw, 1986), comparison of the observed K_m values and their corresponding catalytic efficiencies (k_{cat}/K_m) remains valid since the three aldopentoses in question contain similar levels (0.02–0.03%) of free aldehyde (Hayward & Angyal, 1977).

Table 4: Apparent Kinetic Constants of Wild-Type and Mutant H110A Human Aldose Reductase for Xylose Isomers[a]

	wild type			H110A			H110Q		
	K_m (mM)	k_{cat}	k_{cat}/K_m	K_m (mM)	k_{cat}	k_{cat}/K_m	K_m (mM)	k_{cat}	k_{cat}/K_m
D-xylose	7.4	0.4	54	1340	0.017	0.013	861	0.054	0.063
L-xylose	111	0.23	2.1	360	0.0012	0.003	1190	0.0065	0.0059
D-lyxose	2630	0.16	0.06	2740	0.005	0.002	506	0.0075	0.014
k_{cat}/K_m ratio									
D-xylose/L-xylose			26			4			11
D-xylose/D-lyxose			900			7			5

[a] k_{cat} (s^{-1}); k_{cat}/K_m (M^{-1} s^{-1}); standard deviation <20%.

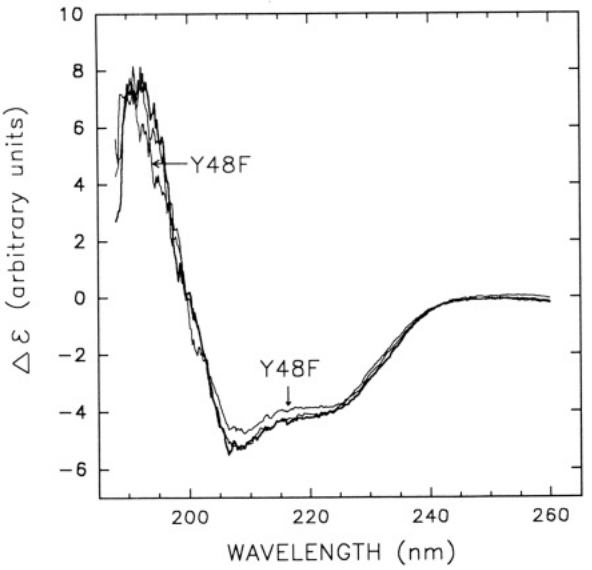

FIGURE 1: Comparison of circular dichroism spectra of recombinant wild-type and mutant aldose reductases. The wild-type enzyme is represented by a thick line, and the mutant enzymes (H110A and Y48F) are represented by thin lines.

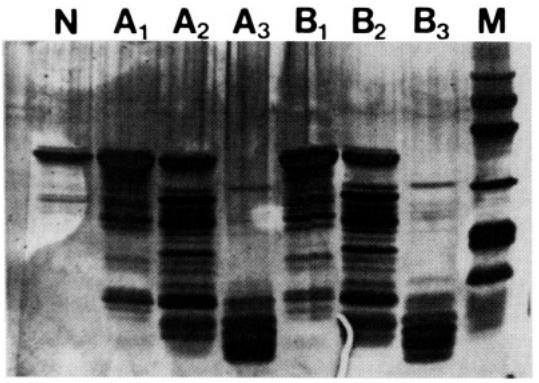

FIGURE 2: Polyacrylamide gel electrophoretogram in the presence of sodium dodecyl sulfate of proteolytic digests of recombinant wild-type (A) and Y48F mutant (B) aldose reductases. The undenatured proteins were digested for 15 min as described in Materials and Methods using either endoproteinase Glu-C (1), endoproteinase Lys-C (2), or alkaline protease (3). Undigested wild-type protein was run in lane N, and molecular mass marker proteins were run in lane M (97.4, 66.2, 45.0, 31.0, 21.5, and 14.4 kDa, respectively).

wild-type, Y48F, and another mutant enzyme, H110A, which has far less than 0.1% of the wild-type enzyme activity (k_{cat}/K_m). The spectra of the three proteins are virtually superimposable. Partial proteolytic digestions by three different proteases under nondenaturing conditions also failed to show any difference in tertiary protein folding structure (Figure 2) between the three proteins.

The Y48H mutant enzyme retains some detectable activity with the k_{cat} reduced to 2.2% and 2.4% of wild-type values for DL-glyceraldehyde and *p*-nitrobenzaldehyde, respectively. As compared to the wild-type enzyme, the K_m values are increased 3550- and 25-fold, respectively, and the k_{cat}/K_m values, relative to wild type, are thus extremely small, 10^{-5} and 10^{-3}, respectively. The Y48S mutant gave similar results for DL-glyceraldehyde (k_{cat} decreased to 2.2% of wild type and K_m increased 3200-fold), although the k_{cat} for *p*-nitrobenzaldehyde decreased much further to 0.005% and the K_m increased 220-fold. These data suggest that the serine mutation creates a particularly unfavorable environment for hydrophobic substrates.

Inhibition of Y48H Mutant Enzyme Activity by Citrate. The wild-type aldose reductase enzyme was shown in the preceding paper (Harrison et al., 1994) to be inhibited by citrate, with inhibition being uncompetitive with respect to the aldehyde in the forward direction ($K_{ii} = 0.17 \pm 0.09$ mM) at pH 5 and competitive with respect to the alcohol in the reverse reaction. The inhibition is pH-dependent and is less pronounced at pH 7, with an inhibition constant $K_{ii} = 9.4 \pm 0.6$ mM with DL-glyceraldehyde and 9.9 ± 0.4 mM with D-xylose as a substrate. The Y48H mutant enzyme also displays inhibition by citrate at pH 5.0 that is uncompetitive with respect to DL-glyceraldehyde ($K_{ii} = 20 \pm 5$ mM), albeit much less potent than for the wild-type enzyme. The difference in K_{ii} values corresponds to 118-fold more potent inhibition by citrate of the wild-type relative to the Y48H enzyme at pH 5. This ratio can be contrasted with the 3000-fold preference of the wild-type enzyme active site for interaction with DL-glyceraldehyde, estimated from the ratio of K_m values for the two enzymes in the plateau region of the k_{cat}/K_m pH profiles (pH ~7). There was no detectable inhibition by citrate of the Y48H mutant at pH 7.

pH Profiles of Wild-Type and Mutant Enzymes. The pH profiles for the k_{cat} and k_{cat}/K_m of the wild-type and Y48H mutant enzymes are distinctly different over the pH range from 5 to 10 (Figure 3). Table 5 lists the pK and Y_{max} values determined from fits of the experimental data to the appropriate equation. Wild-type aldose reductase turnover (k_{cat}) goes through a wave, decreasing progressively with increasing pH. Data analysis, using eq 6 (Materials and Methods), gave values for $pK_1 = 7.0 \pm 0.3$, the point where the initial break to a slope of −1 occurs, $pK_2 = 8.4 \pm 0.4$, the point where the rate levels out, and $pK_3 = 9.7 \pm 0.6$, the point where the profile again breaks to a slope of −1. The difference in plateau values for the wave occurring above pH 7.0, which is equal to the apparent pK values ($pK_2 - pK_1 = 1.4$ log units), indicates that the deprotonation of the enzymic group with pK = 7.0 leads to a 25-fold decrease in k_{cat}. Since the rate-limiting step in the reaction cascade was shown to involve a conformational change of the enzyme during $NADP^+$/NADPH exchange (Grimshaw et al., 1989; Kubiseski et al., 1992), we conclude that the decrease in k_{cat} above pH 7 results from a decrease in the rate of the cofactor exchange reaction. The k_{cat}/K_m for wild-type enzyme displays a single breakpoint on the basic side, with $pK_1 = 8.4 \pm 0.1$, as determined from a

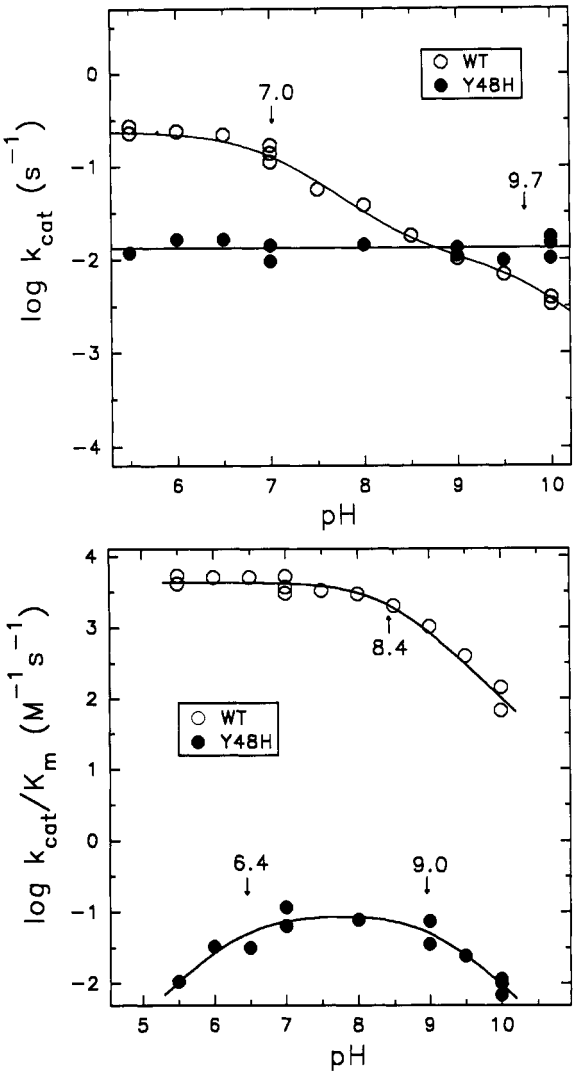

FIGURE 3: Effect of pH on log k_{cat} (A, top) and log k_{cat}/K_m (B, bottom) for the reduction reaction of DL-glyceraldehyde catalyzed by wild-type (open circles) and Y48H (closed circles) mutant aldose reductases. pK_a values, noted with arrows, were obtained by fitting the appropriate equation to the experimental data (see Materials and Methods).

Table 5: pK Values from pH Profiles of k_{cat} and k_{cat}/K_m for Wild-Type and Y48H Aldose Reductase

parameter	eq	pK_1	pK_2[a]	pK_3	Y_{max}
wild type					
log k_{cat} (s^{-1})	5	7.0 ± 0.3	8.4 ± 0.4	9.7 ± 0.6	0.24 ± 0.03
log k_{cat}/K_m (M^{-1} s^{-1})	3	8.4 ± 0.1			4300 ± 300
Y48H					
log k_{cat} (s^{-1})					0.013 ± 0.002
log k_{cat}/K_m (M^{-1} s^{-1})	4	6.4 ± 0.2	9.0 ± 0.1		0.090 ± 0.02

[a] pK_2 is not a true pK_a but rather an inflection point marking the end of the 25-fold decrease in k_{cat} above pK_1 = 7.0.

fit of eq 3 to the data. Thus, deprotonation of a single enzymic group (glyceraldehyde substrate is uncharged and NADPH does not ionize in this pH region) leads to a decrease in binding and/or catalysis.

In contrast, the k_{cat} pH profile for the Y48H mutant is essentially flat between pH 6 and pH 10. In fact, above pH 9, k_{cat} for the Y48H mutant exceeds that for the wild-type enzyme. k_{cat}/K_m for Y48H displays a bell-shaped pH profile with a break at both acidic and basic pH and with the basic

Table 6: Primary Deuterium and Solvent Isotope Effects for DL-Glyceraldehyde Reduction

	pH 7.0		pH 10.0	
	wild type	Y48H	wild type	Y48H
$^D(k_{cat})$	0.99 ± 0.02	1.81 ± 0.03	1.04 ± 0.02	2.53 ± 0.03
$^D(k_{cat}/K_m)$	1.82 ± 0.08	1.81 ± 0.03	1.98 ± 0.06	2.53 ± 0.03
$^{D_2O}(k_{cat})$	1.04 ± 0.06	1.06 ± 0.02		
$^{D_2O}(k_{cat}/K_m)$	4.73 ± 0.23	1.06 ± 0.02		

pK value shifted to much higher pH than was found for the wild-type enzyme. Analysis using eq 4 gave values of pK_1 = 6.4 ± 0.2 and pK_2 = 9.0 ± 0.3 for the Y48H mutant. The break at pH 9.0 seen in the k_{cat}/K_m profile for Y48H does not appear in the k_{cat} pH profile, suggesting that aldehyde substrate binds only to the correctly protonated form of the E–NADPH binary complex. The difference in pH behavior of k_{cat} seen for the Y48H enzyme suggests that the rate-limiting step for this mutant is not the same as that for the wild-type enzyme; i.e., cofactor exchange is not rate-limiting.

Localization of the Rate-Limiting Step in the Y48H Mutant Enzyme. Comparison of the primary deuterium isotope effects for the wild-type and mutant Y48H enzymes (Table 6), determined by using NADPH and NADPD with DL-glyceraldehyde as the substrate, provides evidence for the rate-limiting step in the catalytic cascade in Y48H. In the wild-type enzyme, there is a significant primary isotope effect on k_{cat}/K_m (1.82 ± 0.08) but none on k_{cat} (0.99 ± 0.02). This is consistent with the rate of $NADP^+$ release (or the E–$NADP^+$ isomerization step preceding $NADP^+$ release) being the slowest step for the overall forward reaction of aldehyde reduction in the wild-type enzyme. However, hydride transfer is partially rate-limiting for the catalytic sequence, which includes all steps between the addition of aldehyde and the release of the alcohol product. In the Y48H mutant enzyme, the isotope effects on k_{cat} and k_{cat}/K_m are both significantly different from 1.00 and are equal (1.81 ± 0.03), suggesting that the sequence of steps containing the hydride-transfer step has now become rate-limiting and that the value of 1.81 is, in fact, the intrinsic isotope effect on hydride transfer reduced only by internal commitments.

The wild-type enzyme shows no solvent isotope effect on k_{cat} but shows a large solvent isotope effect on k_{cat}/K_m (4.73 ± 0.23), suggesting that the proton transfer which must occur during the conversion of aldehyde to alcohol is also a slow step in the catalytic process. In contrast, the Y48H mutant shows essentially no solvent isotope effect on either k_{cat} or k_{cat}/K_m (1.06 ± 0.02), indicating that the relative contribution of proton transfer to the rate limitation of the catalytic cascade is much less important for the Y48H mutant. In other words, proton transfer is relatively much easier than hydride transfer for the Y48H mutant than it is for the wild-type enzyme. The data implicate the hydride-transfer step as the major rate-limiting step in the Y48H mutant enzyme and suggest that Tyr48 plays a critical role in the proton-transfer step.

Crystallographic Structure of the Y48H Mutant Aldose Reductase Enzyme. Many attempts to crystallize the Y48F mutant, under a wide variety of conditions known to crystallize wild-type aldose reductase readily, have failed. However, we were able to crystallize the Y48H enzyme mutant using conditions identical to those previously used to crystallize the wild-type enzyme. We obtained Y48H protein crystals that diffracted to better than 1.6-Å resolution. As in the case of the wild-type aldose reductase crystals, the Y48H crystals belong to the space group $P2_12_12_1$ with unit cell dimensions

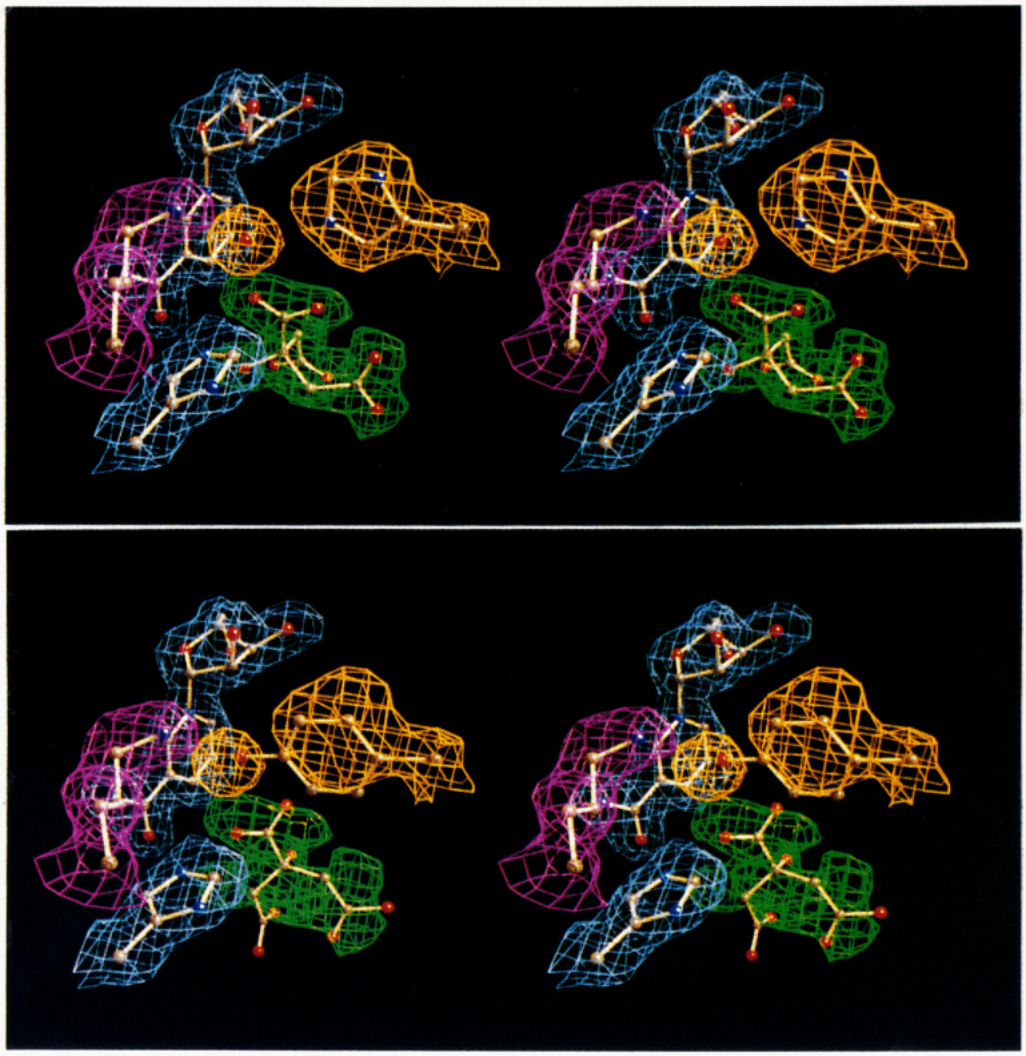

FIGURE 4: Stereoview of the electron density of the active site residues of the Y48H mutant enzyme contoured at 0.8σ above the mean density in a $3|F_o| - 2|F_c|$ difference Fourier map. A ball-and-stick model of the residues is enclosed within the electron densities. The view is from underneath the active site cavity looking upward toward the solvent. (A, top) The citrate (green) is within the active site pocket. His48 (yellow density), via its Nϵ group, is within hydrogen-bonding distance to the associated water molecule (yellow density), which is in turn hydrogen bonded to the Nζ of Lys77 (magenta density). His110 (blue density, lower left corner) and the nicotinamide ring of $NADP^+$ (blue) complete the catalytic site. (B, bottom) Superimposition of the wild-type ball-and-stick model on the electron density of the Y48H active site, based on the least-squares fit of all the α-carbons of both models. Note that the wild-type Tyr48 hydroxyl group situates within the electron density of the water molecule (0.5 Å). Also note that, compared with the Y48H citrate coordinates, the wild-type citrate molecule is rotated around an axis described by its C3 and carboxylate carbon.

of $a = 49.99$ Å, $b = 67.14$ Å, and $c = 92.07$ Å and contained one molecule per asymmetric unit.

The refined 1.8-Å crystal structure of the Y48H mutant enzyme shows that it maintains the α/β TIM-barrel configuration without any significant changes from the wild-type enzyme crystal structure. In particular, the location and interactions of the loop spanning residues 213–228, which covers and secures the NADPH, do not differ from the wild-type structure. The residues composing this loop continue to have the highest average individual *B*-factors in the protein structure. As might be expected, the main difference between the wild-type and the Y48H structures is in the active site pocket. Again, an electron density for citrate is found (Figure 4A), which is better resolved with lower *B*-factors than for the wild-type structure described in the accompanying paper (Harrison et al., 1994). In the wild-type structure, the C3-carboxylate of citrate is located near the C4 of nicotinamide, the Nϵ of His110, and the OH of Tyr48. In the mutant structure this carboxylate remains in the same position relative to the nicotinamide and His110. The remainder of the citrate molecule has rotated about an axis described by C3 and the carboxylate carbon (Figure 4). These findings suggest that the previously described (Harrison et al., 1994) anion binding site delineated by the 4-*pro-R* hydrogen of the nicotinamide, His110, Tyr48, and Lys77, continues to be maintained despite the replacement of tyrosine with histidine. The altered positions of the terminal carboxylates of citrate indicate that some changes in charge distribution have taken place.

The Y48H mutant structure shows clear electron densities for the histidine side chain and a new water molecule, which fill the space formerly occupied by Tyr48 (Figure 4A). In particular, the new water molecule is located in the space previously occupied by the hydroxyl group of tyrosine and is within hydrogen-bonding distance to the ammonium side chain of Lys77 and the Nϵ2 of His48. Figure 4B shows the wild-type coordinates fitted to the $2|F_o| - |F_c|$ electron density map of the Y48H structure which clearly indicates the hydroxyl of Tyr48 centered in the new water molecule. This finding suggests that the water molecule is the proton donor during catalysis in the Y48H mutant and supports the hypothesis that Tyr48 is indeed the proton donor during catalysis in the wild-type aldose reductase.

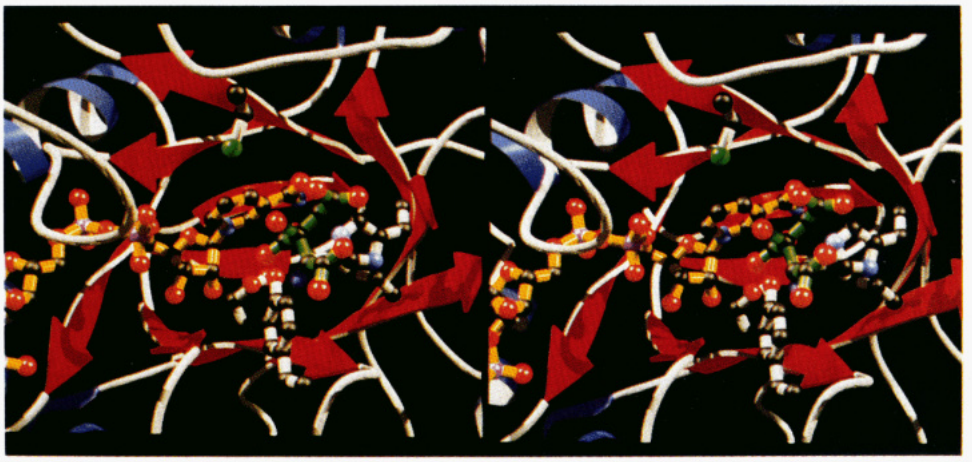

FIGURE 5: Close-up stereoview of a ribbon representation of the active site pocket of aldose reductase. The view is from the solvent side looking into the bottom of the pocket. $NADP^+$ (yellow) is shown with the C4 (arrowhead) of its nicotinamide in the center of the view. The backbone diphosphate and the C2′ phosphate of the adenosine ribose are shown in magenta. Tyr48 (black and white) is at 6 o'clock with its hydroxyl group within hydrogen-bonding distance of the underlying Lys77 (blue), which is in turn in salt-bridge linkage to Asp43, underlying and to the left of Tyr48. His110 (blue) is at 3 o'clock. Citrate (green) is in the active site pocket with its C3 carboxylate in the plane of a triangle formed by the C4 of nicotinamide, the OH of Tyr48, and the Nϵ of His110. Cys298 (green) is at the top of the figure.

DISCUSSION

Aldose reductase is a broad-spectrum NADPH-dependent reductase with substrate specificity ranging from aldoses and ketoses to hydrophobic corticosteroids and xenobiotic aldehydes. The catalytic efficiencies for these substrates vary widely, although the enzyme appears to be finely attuned to the prevailing individual substrate levels. The atomic structure of aldose reductase indicates that it is an α/β barrel enzyme with the NADPH cofactor enfolded across the C-terminal end of the barrel by a loop of residues. Only two segments of the extended NADPH cofactor are exposed to the solvent, a portion of the adenosine phosphoribose end and the nicotinamide ring end. The nicotinamide lies at the bottom of a deep active site pocket with its 4-*pro-R* hydrogen exposed to the solvent. The extremely nonpolar pocket is lined with a large number of hydrophobic residues, some of which are contributed by the loop enfolding the NADPH. Two putative catalytic residues, His110 and Tyr48, along with the 4-*pro-R* hydrogen of the nicotinamide form a triangle at the bottom of the active site pocket (Figure 5). An indication of the substrate binding mechanism is provided by the identification of citrate, bound at the center of the plane of the equilateral triangle (Figure 5) in aldose reductase crystals at pH 5. Citrate, used in the crystallization buffers, is an uncompetitive inhibitor of aldose reductase with respect to aldehyde substrates in the forward direction and a competitive inhibitor with respect to the alcohol in the backward reaction. The inhibitor binding site is a positively charged anion well formed by Asp43/Lys77, Tyr48, His110, and the nicotinamide ring at the bottom of the active site pocket (Harrison et al., 1994). The proximity of the positively charged Lys77 perturbs the pK_a of Tyr48 which would facilitate proton transfer.

The catalytic mechanism of aldose reductase involves binding of the substrate to the E–NADPH complex with subsequent hydride transfer from the nicotinamide ring to the carbonyl group. A proton must be added to the carbonyl oxygen sometime during the reaction to complete the conversion of aldehyde to alcohol. The alcohol product is then released, and the enzyme begins a complex conformational change whereby the holding loop opens to exchange $NADP^+$ for NADPH and closes again to repeat the cycle. In the proposed mechanism, either His110 or Tyr48 could serve as the proton donor, although the latter seems to be the more likely candidate from the results of the experiments reported herein.

Stereochemical Orientation of Substrates by His110. His110 is the only polar residue in the large and extremely hydrophobic active site pocket (Wilson et al., 1992). Modeling studies using methylglyoxal or acetol (Harrison et al., 1994), based on the crystallographic structure of the citrate–enzyme complex, suggested that His110 directs the stereochemistry of the hydride attack. Furthermore, it may have a role in orienting such diverse substrates as aldols and arylalkylaldehydes. In this study, we show that the overall enzymic activities of the His110 mutants are affected to a lesser extent than the Tyr48 mutants. Moreover, the nature of the histidine replacement affected not only the overall activity but the substrate specificity as well. Thus, a polar substitution, such as in H110Q, retained roughly equivalent catalytic efficiency for reduction of either DL-glyceraldehyde or *p*-nitrobenzaldehyde. The H110A mutant, on the other hand, displayed a 150-fold preference in k_{cat}/K_m terms for reduction of the more hydrophobic substrate (6-fold better than H110Q with *p*-nitrobenzaldehyde). These findings suggest that recognition of a polar substrate, in contrast to a hydrophobic one, requires the presence of a polar residue at position 110. Thus, His110 may be involved in the binding or orientation of highly polar substrates. It is interesting to note that the preferred configuration of sugar aldoses (2-D- and 3-L-OH) as substrates for aldose reductase-mediated reduction is exactly that found in the physiologically relevant isomers, D-glucose (C6), D-xylose (C5), and D-glyceraldehyde (C3), consistent with a detoxification role for this enzyme in normal metabolism (Grimshaw, 1992).

This hypothesis was further examined by testing the ability of wild-type and H110A mutant enzymes to distinguish between D-xylose and its stereoisomers, L-xylose and D-lyxose. The wild-type enzyme clearly distinguishes between D-xylose and L-xylose and between D-xylose and D-lyxose (25- and 900-fold better catalytic efficiencies, respectively). These results clearly show the importance of both the C2- and C3-hydroxyls in allowing the proper orientation of aldose substrates within the enzyme active site. Substitution of alanine in the H110A mutant results in an initial 4100-fold reduction in k_{cat}/K_m for the preferred D-xylose substrate. However, once this key alignment residue is removed, subsequent changes at either

C2 (D-xylose vs D-lyxose) or C3 (D-xylose vs L-xylose), have little effect, showing only a 4–6-fold additional decrease in catalytic efficiency. The H110Q mutant displays a similar trend in stereospecificity. Thus, although the initial reduction in catalytic efficiency is somewhat less (860-fold) when glutamine is substituted, essentially the same magnitude of effects is seen for the C2 and C3 isomers. We conclude, therefore, that His110 plays an important role in directing the stereochemical orientation of polar 2-hydroxyaldehyde substrates and thus is unlikely to be the proton donor in the catalytic reaction.

Tyr48 Is the Proton Donor in the Reduction Reaction. Tyr48 is the most likely candidate to be the proton donor, functioning as a general acid catalyst to facilitate the hydride transfer from NADPH to the carbonyl carbon of the substrate. Mutation of this residue to phenylalanine, which conserves the hydrophobic properties and spatial fit of a tyrosine residue yet eliminates the possibility of any general acid catalysis by removing the tyrosyl hydroxyl group, leads to a completely inactive enzyme. On the other hand, two other substitutions, Y48S and Y48H, where both the hydrophobic character and the steric bulk of the residue were dramatically altered but the hydrogen-bonding ability of the hydroxyl moiety was partially retained, produced mutant enzymes that were slightly active. Because the loss of activity could arise from a gross conformational change rather than from any specific effect of the particular mutation on catalysis, we sought to establish that the overall three-dimensional structure of these mutants and especially their nucleotide and substrate binding sites remained intact.

CD spectra, nucleotide binding constants, and proteolytic fingerprints of nondenatured mutant enzyme protein did not suggest any significant alteration of the tertiary structure in the mutant proteins. In fact, binding constants for NADPH and $NADP^+$ (Ehrig et al., unpublished results) in the Y48F and Y48H mutants were virtually identical to those determined for the wild-type enzyme, indicating that the complex interaction with the nucleotide is unaffected. The most convincing evidence of an intact tertiary structure was produced by X-ray crystallographic analysis of the Y48H mutant which revealed a structure surprisingly similar to the wild-type protein. The major difference between the wild-type and the Y48H structures is a water molecule, hydrogen bonded between the Nζ of Lys77 and the Nϵ of His48, filling the space normally occupied by the hydroxyl of Tyr48. A postulated change in charge distribution is indicated by a rotation of the citrate ligand within the active site pocket (Figure 4). It is thus reasonable to assume that the inactive Y48F mutant, a protein we have been unable to crystallize so far, has an intact tertiary structure as well. We believe that our inability to crystallize Y48F in our standard citrate buffer results from the inability of the phenylalanine mutation to interact with the positively charged Lys77, resulting in an incomplete formation of the positively charged anion well necessary for the binding of citrate or substrates. The fact that mutation of Lys77 to methionine produces an inactive enzyme is consistent with this postulated role for Lys77.

The Y48H crystal structure suggests that the water molecule positioned in the space normally occupied by the hydroxyl group of Tyr48 in the wild-type enzyme is recruited to serve as the proton donor in the catalytic reduction reaction. Like the hydroxyl of Tyr48, the water molecule is within hydrogen-bonding distance to the positively charged Nζ of Lys77, and its pK_a is presumably perturbed downward, thus facilitating proton transfer. The Lys77 positive charge is itself perturbed to a higher pK_a by forming a salt bridge with the neigboring Asp43 (2.8 Å).

Catalytic Mechanisms of the Wild-Type and Y48H Enzymes. Comparison of the pH profiles for the kinetic parameters and the primary deuterium isotope effects further clarify the role of Tyr48 in catalysis of the wild-type enzyme. The rate-limiting step in the reaction cascade for the wild-type enzyme at pH 7 has already been shown to involve a conformational change of the enzyme during $NADP^+$/NADPH exchange (Grimshaw et al., 1989; Kubiseski et al., 1992). This is consistent with the value of $^Dk_{cat} = 1.00$ reported previously (Bohren et al., 1992) and observed here (Table 6). Above pH 7, k_{cat} goes through a wave, decreasing roughly 1.4 log units (25-fold) by pH 9. However, even at pH 10, the value of $^Dk_{cat}$ is still not significantly different from 1.00, which implies that the decrease in k_{cat} above an apparent pK of 7 must be a direct result of a change in the net rate of nucleotide exchange. The identity of the wild-type enzyme group whose deprotonation leads to the drop in k_{cat} has not yet been established.

The pH variation of k_{cat}/K_m for the wild-type enzyme is much simpler, displaying a single enzymic group with an apparent pK of 8.4, which must be protonated for binding and/or catalysis. In addition, $^Dk_{cat}/K_m$, the primary deuterium isotope effect on k_{cat}/K_m, remains essentially constant over the pH range from 7 to 10, which means that DL-glyceraldehyde cannot be a "sticky" substrate. If it were, the $^Dk_{cat}/K_m$ value would be expected to increase above the apparent pK at 8.4 as the net rate of the forward hydride-transfer step decreased relative to the rate of aldehyde release (Cook, 1991). The isotope effect results also imply that 8.4 is the true pK value for the enzymic group(s) in the E–NADPH complex and that the observed value of 1.82 for $^Dk_{cat}/K_m$ is equal to the intrinsic isotope effect reduced only by internal commitments. The fact that the same enzymic group does not appear in the log k_{cat} versus pH profile[5] confirms that aldehyde binding to form the ternary E–NADPH–aldehyde complex locks the enzyme in the correct protonation state.

On the basis of the crystal structure, we would ascribe the pK of 8.4 seen in the k_{cat}/K_m profile to Tyr48. As noted above, the proximity of Asp43 to Lys77 is likely to perturb the pK of the latter toward higher pH, stabilizing the salt bridge between $Asp43^-$ and $Lys77^+$. Similarly, the protonated cationic Lys side chain is in position to donate a hydrogen bond to the Tyr48 hydroxyl moiety, thereby facilitating ionization of the latter. An apparent pK of 8.4 for Tyr48 thus represents a 2 pK unit shift from the pK of 10.5 seen for a free tyrosyl hydroxyl group in solution. Note also that the overall charge on the active site is neutral, composed of $Asp43^-$/$Lys77^+$/$Tyr48^0$/$NADPH^0$ (at the nicotinamide ring). As we will see below, the same overall net charge is optimal for catalysis by the Y48H mutant enzyme as well.

The solvent isotope effect results point to an important role for proton transfer in the catalytic cascade for the wild-type enzyme. Again, $^{D_2O}k_{cat}$ is equal to 1.0 as expected for rate-limiting nucleotide exchange. However, the value for $^{D_2O}k_{cat}/K_m$ of 4.7 suggests that proton transfer is quite slow for the wide-type enzyme and probably contributes significantly more

[5] The pK observed at 9.7 for k_{cat} cannot be due to the same pK 8.4 group seen in the k_{cat}/K_m profile for the following reason: The value of $^Dk_{cat}$ is 1.00 because the forward commitment factor, C_{Vf}, consisting of the ratio of the rate of hydride transfer to the much slower net rate of $NADP^+$ release, is quite large (Cook, 1991). Given $^Dk_{cat}/K_m = 1.82$, C_{Vf} must be at least 10 at pH 7 and increase to 250 by pH 9. Because C_{Vf} also affects the apparent pK in the log k_{cat} versus pH profile, as apparent pK = pK + log(1 + C_{Vf}), the apparent pK value must be >10.5!

to the rate limitation of the catalytic cascade than does hydride transfer.

If we assume values for the intrinsic isotope effects in the hydride-transfer and proton-transfer transition state(s), we can speculate as to what extent each might contribute to the overall rate limitation of a stepwise reaction sequence; e.g., proton transfer precedes hydride transfer. If we use the value of 5.3 for ^{D}k, the intrinsic isotope effect on hydride transfer based on that determined for glucose-6-phosphate dehydrogenase (Hermes & Cleland, 1984), and the value of 8 for ^{D_2O}k determined for the solvent isotope effect on k_{cat}/K_m of the Y14F mutant of Δ^5-3-ketosteroid isomerase (Xue et al., 1991), then a simple calculation would suggest about 15% rate limitation by hydride transfer and about 45% rate limitation by proton transfer, with the remainder contributed by other steps comprising k_{cat}/K_m. If, on the other hand, the reaction is concerted, the observed isotope effects for wild-type enzyme would suggest a fairly symmetrical transition state with respect to proton transfer and a relatively less symmetrical transition state with respect to hydride transfer (i.e., either early or late, relative to proton transfer). In either case, proton transfer is a significant contributor to the rate limitation of k_{cat}/K_m for the wild-type enzyme.

The pH profiles for the kinetic parameters and isotope effects are quite different for the Y48H mutant, supporting the proposed change from a tyrosyl hydroxyl group as the general acid catalyst in the wild-type enzyme to a histidine-assisted water moiety in the Y48H mutant. First, log k_{cat} remains constant over the pH range from 5.5 to 10, while k_{cat}/K_m displays a bell-shaped profile with optimal catalysis and/or binding occurring when an enzymic group with pK 6.4 is unprotonated and a second group with pK 9.0 is protonated. On the basis of the results for the wild-type enzyme and the crystal structure for the Y48H mutant, we ascribe the pK 9.0 to the constellation comprised of Asp43/Lys77/His48/H_2O and the pK 6.4 to His48. Specifically, the break in k_{cat}/K_m at pH 9 most likely represents deprotonation of Lys77 and the break at pH 6.4, protonation of His48. Just as was observed for the wild-type enzyme, the overall charge on the enzyme active site at the optimal protonation state for the Y48H mutant is neutral, consisting of $Asp43^{-}/Lys77^{+}/His^{0}$–$H_2O$/$NADPH^{0}$.

The isotope effect results also point to key differences between the wild-type and Y48H mutant enzymes. The primary deuterium isotope effects on k_{cat} and k_{cat}/K_m for the Y48H mutant are equal in magnitude and significantly different from 1.0, indicating that the sequence of steps comprising $k_{cat}/K_{m(aldehyde)}$, which includes all steps from the addition of aldehyde to E–NADPH through the release of alcohol product, is now rate-limiting for the overall reaction. In other words, nucleotide release or "exchange" cannot be rate-limiting for the Y48H mutant aldose reductase. Moreover, the Y48H mutant shows essentially no solvent isotope effect on either k_{cat} or k_{cat}/K_m ($^{D_2O}k_{cat} = {}^{D_2O}k_{cat}/K_m = 1.06$). Thus, despite the fact that the $^{D}k_{cat}/K_m$ values for hydride transfer are virtually identical for the two enzymes at pH 7, proton transfer must contribute essentially nothing to the overall rate limitation of the catalytic cascade in the Y48H mutant enzyme.

Similar values of $^{D}k_{cat}/K_m$ for wild-type and Y48H mutant enzymes at pH 7 could indicate a similar extent of rate limitation by the hydride-transfer step. However, without information on the intrinsic ^{D}k values for the two enzymes, meaningful comparisons are not possible. Sweet and Blanchard (1991) have shown that the intrinsic hydride-transfer isotope effect for glutathione reductase varies depending on the nature of the nucleotide cofactor, ranging from 1.4 for NADH to 4.8 for the 3-acetylpyridine analogue. It might therefore be expected that the intrinsic effect would also depend on the nature of the enzyme active site.

In any case, the fact that $^{D}k_{cat}/K_m = 1.8$ and $^{D_2O}k_{cat}/K_m = 1.0$ means that the Y48H enzyme must *de facto* proceed via a stepwise mechanism, with rapid proton transfer occurring either before or after hydride transfer. Above the break in k_{cat}/K_m at pH 9, the values of both $^{D}k_{cat}$ and $^{D}k_{cat}/K_m$ for the Y48H mutant increase from 1.8 to 2.5, reflecting a further unmasking of the intrinsic isotope effect. Thus, above pH 9 some step comprising the internal commitment (Cook, 1991) must change to allow more rate limitation by and, therefore, more expression of the isotope effect on the hydride-transfer step. Slowing of the proton-transfer rate, which might be expected to occur at high pH, cannot be the cause, as this would result in a *decrease* in rate limitation by the hydride-transfer step and a *decrease* in observed $^{D}k_{cat}/K_m$.

The aldose reductase active site is ideally suited to transfer a hydride from nicotinamide to the aldehyde substrates. The very hydrophobic pocket effectively excludes water in the presence of ligand. The Asp43–Lys77–Tyr48 system of providing the proton for aldehyde reduction is ideally suited to the type of one-way catalysis that characterizes the aldo–keto reductase superfamily (Grimshaw, 1992). To use a histidine such as is employed in lactate dehydrogenase would mean that, above the pK of 7.5, catalytic effectiveness would be lost. The hydroxyl of Tyr48, modulated by hydrogen bonding with the protonated Lys77, which in turn is maintained by the Asp43 residue, is an ideal configuration to serve as a proton donor over the pH range from 6 to nearly 9, with little loss in catalytic efficiency. By further maintaining an overall neutral charge on the enzyme active site [$Asp43^{-}/Lys77^{+}/Tyr48^{0}$/$NADPH^{0}$ (at the nicotinamide)], this juxtaposition of residues allows for a proton to be transferred to the incipient alcohol moiety while extending the developing negative charge on the tyrosyl hydroxide across the entire three-residue system. This arrangement also suggests why aldose reductase is such a poor alcohol dehydrogenase. Given the apparent pK of this system of near 9, the enzyme cannot get any pull to remove the proton from the alcohol and facilitate the leaving of hydride to form aldehyde.

What then is responsible for the nearly 50 000-fold decrease in catalytic efficiency in DL-glyceraldehyde reduction by the Y48H mutant relative to the wild-type enzyme? Substitution of the Tyr48 hydroxyl with an apparent pK of 8.4 by a water molecule with an effective pK of 13.4 (assuming a 2 pK unit shift analogous to that seen for Tyr48) could potentially account for a 100 000-fold deficit in general acid catalysis. Yet, comparison of the primary deuterium and solvent isotope effects clearly demonstrates that it is hydride transfer that is most affected and not proton transfer. Precise alignment of the carbonyl-containing substrate within the active site undoubtedly contributes a great deal to the catalytic efficiency, as was shown with the various His110 mutants. Structural evidence indicates that while the protein mutant structure is not different from the wild type, it has nevertheless undergone some subtle changes. The Y48H active site now accommodates a new water molecule in place of the tyrosyl hydroxyl of Tyr48, resulting in an overall geometry for hydride transfer that is so unfavorable as to preclude any significant rate limitation by the protonation step. This is evident in part by rotation of the citrate molecule in the Y48H active site pocket as compared to the wild type.

Earlier evidence for the participation of a tyrosine residue(s) at the active site of native bovine lens aldose reductase was based on an observation of rapid inactivation of the enzyme by nitration using 0.2 mM tetranitromethane at pH 8.0 (Doughty et al., 1982). In studies of the closely related enzyme, human aldehyde reductase, the requirement for an enzymic residue with a pK near 8 which must be protonated for aldehyde reduction in the forward direction and unprotonated for alcohol oxidation in the reverse direction was inferred from extensive pH studies (Bhatnagar et al., 1991). On the basis of those results and on chemical modification studies, the putative active site residue was tentatively identified as a histidine. In light of our results, and in view of the extensive sequence homology between human aldehyde and aldose reductase (Bohren et al., 1989), it seems likely that the general acid/general base catalyst in aldehyde reductase will also prove to be a tyrosine residue (Tyr49 in aldehyde reductase).

On the basis of the fact that a majority of classic aldose reductase inhibitors contain either a carboxylic acid moiety or a 5-substituted hydantoin which is negatively charged at physiological pH, it was proposed that such inhibitors interact with a nucleophilic amino acid. This amino acid was tentatively identified as tyrosine by studies with protein modification reagents and molecular orbital calculations (Kador et al., 1985). Our results suggest that the mode of interaction of aldose reductase inhibitors in some manner involves the active site Tyr48 residue.

To our knowledge there are hitherto only two enzymes where tyrosine residues have been shown to serve as a general acid catalyst, namely, β-galactosidase of *Escherichia coli* (Ring et al., 1990) and Δ^5-3-ketosteroid isomerase of *Pseudomonas testosteroni* (Kuliopulos et al., 1989, 1991). The family of the short-chain alcohol dehydrogenases, however, may well utilize a similar catalytic machinery. Each member of this family contains a highly conserved sequence TyrXXXLys (Persson et al., 1991). Recently, the atomic structure of 3α,-20β-hydroxysteroid dehydrogenase from *Streptomyces hydrogenans* revealed that this highly conserved sequence is lining the substrate binding pocket (Ghosh et al., 1991). Mutation of the conserved Tyr (Tyr152) to Phe in *Drosophila* alcohol dehydrogenase and to Ala in human NAD^+-dependent 15-hydroxyprostaglandin dehydrogenase, both members of the short-chain alcohol dehydrogenase family, leads to completely inactive enzymes (Albalat et al., 1992; Ensor et al., 1991). A similar mutation of Tyr to Phe in dihydropteridine reductase, also shown to be a member of this enzyme family, yields an enzyme with less than 0.3% activity (Whiteley et al., 1993). The fact that some members of this enzyme family actually work better as reductases, including the NADPH-dependent 15-hydroxyprostaglandin reductase, better known as carbonyl reductase, and dihydropteridine reductase, suggests that a catalytic mechanism potentially similar to that proposed here for aldose reductase could be operating in this otherwise unrelated family of NAD(P)-dependent oxidoreductases.

ACKNOWLEDGMENT

We thank Daniel Peisach for his development and help in the use of the computer programs that generated Figures 4 and 5. We also thank Ragini Shankar and Stephen Henry for their technical assistance.

REFERENCES

Albalat, R., Duarte, G., & Atrian, S. (1991) *FEBS Lett. 308*, 235–239.

Bohren, K. M., & Gabbay, K. H. (1993) *Adv. Exp. Med. Biol. 328*, 267–277.

Bohren, K. M., Bullock, B., Wermuth, B., & Gabbay, K. H. (1989) *J. Biol. Chem. 264*, 9547–8551.

Bohren, K. M., Page, J. L., Shankar, R., Henry, S. P., & Gabbay, K. H. (1991) *J. Biol. Chem. 266*, 24031–24037.

Bohren, K. M., Grimshaw, C. E., & Gabbay, K. H. (1992) *J. Biol. Chem. 267*, 20965–20970.

Brünger, A. T. (1992) XPLOR SOFTWARE, Yale University, New Haven, CT.

Cleland, W. W. (1963) *Arch. Biochem. Biophys. 67*, 104–137.

Cleland, W. W. (1979) *Methods Enzymol. 63*, 103–138.

Cook, P. F. (1991) in *Enzyme Mechanism from Isotope Effects* (Cook, P. F., Ed.) pp 231–265, CRC Press, Boston, MA.

Doughty, C. C., Lee, S.-M., Conrad, S., & Schade, S. (1982) *Enzymology of Carbonyl Metabolism: Aldehyde Dehydrogenase and Aldo/Keto Reductase*, pp 223–242, Plenum Press, New York.

Dvornik, D. (1987) *Aldose Reductase Inhibition: An Approach to the Prevention of Diabetic Complications* (Porte, D., Ed.) McGraw Hill, New York.

Ensor, C. M., & Tai, H. H. (1991) *Biochem. Biophys. Res. Commun. 176*, 840–845.

Gabbay, K. H. (1973) *N. Engl. J. Med. 288*, 831–836.

Gabbay, K. H., Spack, N., Loo, S., Hirsch, H. J., & Ackil, A. A. (1979) *Metabolism 28*, 471–476.

Ghosh, D., Weeks, C. M., Grochulski, P., Duax, W. D., Erman, M., Rimsay, R. L., & Orr, J. C. (1991) *Proc. Natl. Acad. Sci. U.S.A. 88*, 10064–10068.

Gill, S. C., & von Hippel, P. H. (1989) *Anal. Biochem. 182*, 319–326.

Grimshaw, C. E. (1986) *Carbohydr. Res. 148*, 345–348.

Grimshaw, C. E. (1992) *Biochemistry 31*, 10139–10145.

Grimshaw, C. E., Shahbaz, M., & Putney, C. G. (1990) *Biochemistry 29*, 9947–9955.

Harrison, D. H., Bohren, K. M., Ringe, D., Petsko, G. A., & Gabbay, K. H. (1994) *Biochemistry* (preceding paper in this issue).

Hayward, L. D., & Angyal, S. J. (1988) *Carbohydr. Res. 53*, 13–20.

Judzewitsch, R. G., Jaspan, J. B., Polonsky, K. S., Weinberg, C. R., Halter, J. B., Halar, E., Pfeifer, M. A., Vukadinovich, C., Bernstein, L., Schneider, M., Liang, K. L., Gabbay, K. H., Rubenstein, A. H., & Porte, D., Jr. (1983) *N. Engl. J. Med. 308*, 119–125.

Kador, P. F. (1988) *Med. Res. Rev. 8*, 325–352.

Kador, P. F., Kinoshita, J. H., & Sharpless, N. E. (1985) *J. Med. Chem. 28*, 841–849.

Kubiseski, T. J., Hyndman, D. J., Morjana, N. A., & Flynn, T. G. (1992) *J. Biol. Chem. 267*, 6510–6517.

Kuliopulos, A., Mildvan, A. S., Shortle, D., & Talalay, P. (1989) *Biochemistry 28*, 149–159.

Kuliopulos, A., Mullen, G. P., Xue, L., & Mildvan, A. S. (1991) *Biochemistry 30*, 3169–3178.

Martyn, C. N., Reid, W., Young, R. J., Ewing, D. J., & Clark, B. F. (1987) *Diabetes 36*, 987–990.

Masson, E. A., & Boulton, A. J. (1990) *Drugs 39*, 190–202.

Northrop, D. B. (1977) in *Isotope Effects on Enzyme-Catalyzed Reactions* (Cleland, W. W., O'Leary, M. H., & Northrop, D. B., Eds.) pp 122–152, University Park Press, Baltimore, MD.

O'Brien, M. M., Schofield, P. J., & Edwards, M. R. (1982) *J. Neurochem. 39*, 810–814.

Orr, G. A., & Blanchard, J. S. (1984) *Anal. Biochem. 142*, 232–234.

Persson, B., Krook, M., & Jörnvall, H. (1991) *Eur. J. Biochem. 200*, 537–543.

Poulsom, R. (1986) *Biochem. Pharmacol. 35*, 2955–2959.

Ring, M., & Huber, R. E. (1990) *Arch. Biochem. Biophys. 283*, 342–350.

Salomaa, P., Schaleger, L. L., & Long, F. A. (1964) *J. Am. Chem. Soc. 86*, 1.

Schowen, K. B. J. (1978) in *Transition States of Biochemical Processes* (Gandour, R. D., & Schowen, R. L., Eds.) pp 225–283, Plenum Press, New York.

Stinson, R. A., & Holbrook, J. J. (1973) *Biochem. J. 131*, 719–728.
Stribling, D., Armstrong, F. M., Perkins, C. M., & Smith, J. C. (1989) *J. Diabetic Complications 3*, 139–148.
Sweet, W. L., & Blanchard, J. S. (1991) *Biochemistry 30*, 8702–8709.
Viola, R. E., Cook, P. F., & Cleland, W. W. (1979) *Anal. Biochem. 96*, 334–340.
Wermuth, B. (1985) *Prog. Clin. Biol. Res. 174*, 209–230.
Wermuth, B., Bürgisser, H., Bohren, K. M., & von Wartburg, J.-P. (1982) *Eur. J. Biochem. 127*, 279–284.
Whiteley, J. M., Xuong, N. H., & Varughese, K. I. (1993) in *10th International Symposium on the Chemistry and Biology of Pteridines and Folates*, Plenum, New York (in press).
Wilson, D. K., Bohren, K. M., Gabbay, K. H., & Quiocho, F. A. (1992) *Science 257*, 81–84.
Xue, L., Talalay, P., & Mildvan, A. S. (1991) *Biochemistry 30*, 10858–10865.